Izvestiya, Atmospheric and Oceanic Physics Vol. 23, No. 7, 1987
UDC 551.513

Laboratory and Theoretical Study of Stationary Rossby Waves Above Isolated Barriers in an Annulus

M. V. KURGANSKIY, I. A. PISNICHENKO AND YU. L. CHERNOUS'KO

Institute of Atmospheric Physics, USSR Academy of Sciences

Laboratory study is carried out on stationary Rossby waves due to fluid flow around isolated barriers in a rotating annulus with a sloping bottom (to produce the beta-effect). The interaction between Rossby waves caused by two identical barriers placed at a certain distance from each other along the flow is studied as a function of the distance between them. The laboratory experiments are in satisfactory agreement with the results of a simple linear resonance theory.

The influence of mountains on atmospheric motions of various scales is a pressing problem for dynamic meteorology, and an extensive literature has been devoted to this problem, including the exhaustive reviews [1, 2]. In previous research along with theoretical and numerical modeling and direct full-scale observations, hydrodynamic experiments in the laboratory play an important role.

Two basic kinds of experiments are clearly evident in all of the actual experiments that have been done. First, there are experiments in which a barrier is towed in a rotating channel [3]. In the second type of experiments a fluid flow is generated by some method against a stationary (relative to the walls of the container) barrier by blowing air above the fluid surface [4] or by rotating the annulus part of the channel bottom [5], or by a sudden change in the angular rotation rate for the channel [6]. However, the flow picture formed in this way is either not completely stationary [3, 6] or the oncoming flow has large vertical and horizontal velocity shear [4, 5].

This paper investigates laboratory work on stationary Rossby waves caused by fluid flow around isolated barriers in a rotating annulus with a sloping bottom. The method of mass sources and sinks realized in [7 -9] is used to produce the oncoming flow. In this case the oncoming flow is completely stationary and has a slight variation with the vertical coordinate. This has made it possible to investigate the interaction between Rossby waves formed by two identical barriers in the channel (depending on the distance between them), which had not been done previously, and has resulted in a satisfactory theoretical interpretation of the results using a simple linear resonance theory.

DESCRIPTION OF THE EXPERIMENTS AND RESULTS

The experimental arrangement is a rotating platform on which is placed an annulus with outer wall radius b = 14.8 cm and width $D = b - a$ = 9.8 cm (where a is the radius of the inner wall of the channel). The angular velocity of rotation for the platform Ω can vary smoothly in the range from 1.5 to 7 sec^{-1}. In order to model the beta-effect the channel bottom has a conical shape, and the tangent of the inclination of the botto γ is 0.43. For large channel rotation rates t parabolicity of the free fluid surface is taken into account by replacing tg γ = 0.43 by the effective value $\mathrm{tg}\,\gamma' = \mathrm{tg}\,\gamma + (2g)^{-1}\Omega^2(b+a)$ (see [10]). The smallest fluid depth in the channel H_{min} was 3.5 cm and was the same for all the experiments. The mass sources were uniformly distributed along the outer wall of the channel, and the sources were distributed along the inner wall. According to the measurements, the azimuthal flow rate

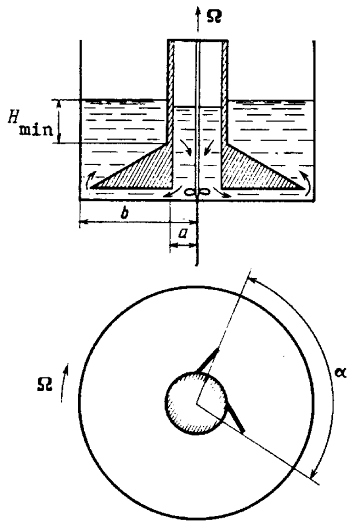

Fig. 1. Diagram of the experiment.

0001-4338/88/2307-0001$18.00/1

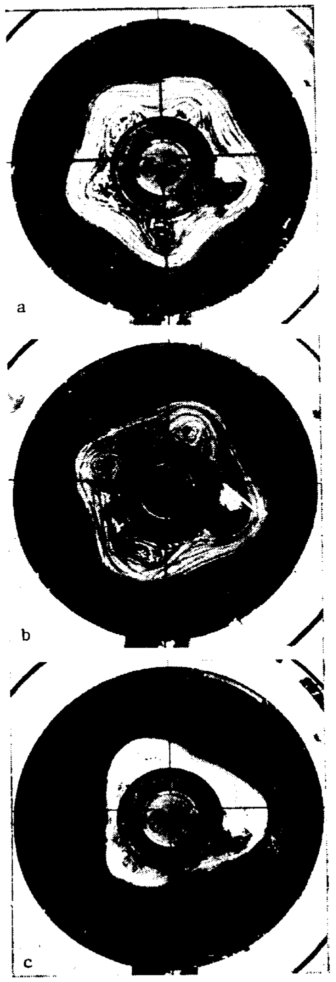

Fig. 2. Flow pictures for a single barrier for Ω = 6.0 sec^{-1} for various fluid delivery rates in the pump Q, g/sec: a) 38, b) 85, c) 98.

profile that resulted was linear, except for narrow zones near the channel walls. The velocity increases from the outer wall to the inner wall. A diagram of the experiment is shown in Fig. 1.

Experiments were first carried out for a flow around an isolated barrier in the shape of a thin plate with vertical generatrices.* The

*The specific shape of the barrier does not play a decisive role in producing the wave picture. Satisfactory results were obtained in preliminary experiments where a spherical segment was used as the obstacle. Nevertheless, it turned out to be convenient to use a vertical wall, deflecting the flow more effectively and occupying a smaller volume in the channel, which is extremely important for two barriers.

Fig. 3. Flow past two barriers for $\alpha \approx 79°$.

angular rotation for the channel and the mean speed for the oncoming flow U (measured in the middle of the channel at a distance $r_0 = (a+b)/2$ = 9.9 cm from the center) were varied respectively in the ranges 1.5 -6.75 cm/sec and 1.0 - 11.3 cm/sec. If the speed of the oncoming flow corresponds to the phase velocity of a normal Rossby mode, then a stationary wave chain is formed with the corresponding symmetry index m (the number of waves fitting in along the channel). We note here that the idea of resonance excitation of Rossby waves by mass point sources and sinks moving with the appropriate speed relative to the fluid was realized in [10, 11].

Our experiments showed the following general rules.

When the channel rotates at a constant angular rate Ω an increase in the mean speed of the oncoming flow U leads to a decrease in m. For example, when Ω = 6.0 sec^{-1} an increase in U by a factor of 2.2 because of a change in the delivery of fluid in the pump leads to a decrease in m from 5 to 3 (Fig. 2).

For a constant pump delivery rate an increase in Ω leads to an increase in m. For example, for a fluid delivery rate of 20 g/sec, which corresponds to $U \approx 2$ cm/sec, the values Ω = 2.06, 3.7 and 5.25 correspond respectively to m = 3, 4, and 5.

The main series of experiments dealt with the study of the flow process around two identical thin plates located a certain distance apart. Experiments were done for Ω = 3.93 cm^{-1} and U = 1.5 -8.5 cm/sec. The distance between the plates is characterized by the angle α between them (Fig. 1); the angle α was varied in the range from 22°40' to 238° in steps of 11°20'. A wave (eddy) chain was formed when the flow moved past the two plates. Since the study was carried out with a fixed value for Ω, the number of eddies was entirely a function of two parameters: the angle between the plates α and the mean velocity of the oncoming flow U, which in this case is determined exclusively by the fluid delivery rate in the pump. The experiments indicated the following.

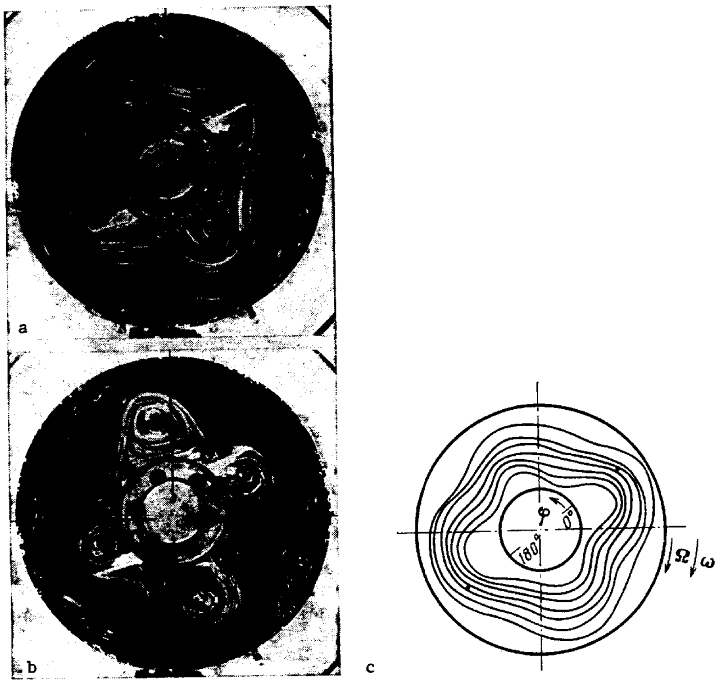

Fig. 4. Pictures for flow past two barriers: a) for $\alpha \approx 182°$, Q = 20 g/sec; b) for $\alpha \approx 182°$, Q = 77 g/sec; c) theoretically computed streamlines for α = 180°, ω = 0.269 sec^{-1}, $\varkappa$ = 0.37 sec^{-2}, and λ = 0.115 sec^{-1}.

For small oncoming flow velocities at $U \approx$ 1.8 cm/sec and angles α, close to 72°, a regular five-eddy structure is observed (Fig. 3).

For $\alpha \approx 180°$ a clear four-eddy structure is observed right up to the largest values for $U \sim 8$ cm/sec. For large U the eddies that are located in the middle between the barriers are much stronger than the eddies found directly at the plates (Fig. 4).

In certain cases, when there is an increase in U an eddy which is initially on the "windward" side of a plate changes to the "leeward" side, but the overall structure does not change.

When U is constant, for certain values $\alpha_0(m)$ small changes in α ($\Delta\alpha \ll 11°20'$) in the neighborhood of α_0 lead to an eddy jumping from one side of a plate to the other (Fig. 5j, k).

MATHEMATICAL MODEL

We consider an annulus with a sloping bottom rotating around a vertical axis. A cylindrical coordinate system is chosen, where r is the radius, φ is the azimuth and z is the altitude. In the quasi-geostrophic approximation the equation for the evolution of the potential vortex has the form (see [10] for more detail)

$$\frac{\partial}{\partial t}\left(\nabla^2\psi - \frac{1}{L_0^2}\psi\right) + [\psi, \nabla^2\psi] + \beta\frac{\partial\psi}{\partial\varphi} = -\lambda\nabla^2\psi - \frac{2\Omega}{H_0}I + F. \tag{1}$$

Here $\psi = gh/2|\Omega|$ is the geostrophic stream function, Ω is the angular rotation rate for the vessel, g is the acceleration due to gravity, $h(r,\varphi,t)$ are small deviations in the height of the free fluid surface from static equilibrium, $\beta = (2\Omega/Hr)dH/dr$, $H(r)$ is the height of a column of fluid under static equilibrium, H_0 is its mean value, $L_0 = \sqrt{gH_0}/2|\Omega|$ is a length scale analogous to the Obukhov scale in the atmosphere, $\lambda = 2C|\Omega|\delta/H_0$ is the coefficient for Ekman friction along the channel bottom, $\delta = \sqrt{\nu/2|\Omega|}$ is the thickness of the Ekman boundary layer, C is a dimensionless parameter on the order of unity, ν is the molecular kinematic viscosity, $I(r)$ describes the distribution and intensity of the external mass sources and sinks, and the $F(r,\varphi)$ are the external vorticity sources. The square brackets denote the Jacobian

$$[A, B] = \frac{1}{r}\left(\frac{\partial A}{\partial r}\frac{\partial B}{\partial\varphi} - \frac{\partial A}{\partial\varphi}\frac{\partial B}{\partial r}\right).$$

For the boundary conditions we assume the periodicity of the solution with respect to φ, the conservation of the velocity circulation at the channel side walls and their impermeability:

$$\psi(r, \varphi+2\pi, t)=\psi(r, \varphi, t),$$
$$\int_0^{2\pi} \frac{\partial\psi}{\partial r} r d\varphi \Big|_{r=a,b} = \text{const}, \quad \frac{1}{r}\frac{\partial\psi}{\partial\varphi}\Big|_{r=a,b} = 0. \tag{2}$$

We set

$$I(r)=I_0 a\delta_-(r-b)-I_0 b\delta_+(r-a) \tag{3}$$

(here δ_- and δ_+ are the asymmetric left and right Dirac delta-functions); in this case

$$\int_a^b I r dr=0,$$

i.e., the fluid mass in the channel is conserved. The value for I_0 is related to the flow rate Q for the pump by the equation

$$I_0=\frac{Q}{2\pi\rho_f ab},$$

where ρ_f is the fluid density.

We parameterize the effect of the plates on the incident flow, placing finite vorticity sources at their ends:

$$F=\varkappa r\delta(\varphi)\delta(r-r_0)+\varkappa r\delta(\varphi-\alpha)\delta(r-r_0), \tag{4}$$

where δ is the symmetric Dirac delta-function. In order to convert to the case for a single barrier, in this formula we should set $\alpha = 0$ and use $\varkappa/2$ instead of $\varkappa$. There is no doubt that it is difficult to obtain explicit expressions for $\varkappa$ using the solution of the hydrodynamics equations. It is not out of the question that parameterization of the barriers in the form of a set of δ-functions or some more complex eddy source is more correct. But for our purposes it is sufficient that the parameterization (4) allows the main experimental results to be explained theoretically.

We represent the stream function field as the sum $\psi=\Psi(r,t)+\psi'(r,\varphi,t)$ and we have for Ψ and ψ' the equations (the tilde denotes averaging with respect to φ):

$$\frac{\partial}{\partial t}\left(\frac{1}{r}\frac{\partial}{\partial r}r\frac{\partial\Psi}{\partial r}-\frac{1}{L_0^2}\Psi\right)-\frac{\partial}{\partial r}\left(\widetilde{\frac{\partial\psi'}{\partial\varphi}\nabla^2\psi'}\right)= -\frac{\lambda}{r}\frac{\partial}{\partial r}r\frac{\partial\Psi}{\partial r}-\frac{2\Omega}{H_0}I+\tilde{F}(r), \tag{5}$$

$$\frac{\partial}{\partial t}\left(\nabla^2\psi'-\frac{1}{L_0^2}\psi'\right)+\frac{1}{r}\frac{\partial\Psi}{\partial r}\frac{\partial\nabla^2\psi'}{\partial\varphi}- -\frac{1}{r}\frac{\partial}{\partial r}\left(\frac{1}{r}\frac{\partial}{\partial r}r\frac{\partial\Psi}{\partial r}\right)\frac{\partial\psi'}{\partial\varphi}+\beta\frac{\partial\psi'}{\partial\varphi}=-\lambda\nabla^2\psi'+F'(r,\varphi), \tag{6}$$

$$\tilde{F}=\frac{\varkappa}{\pi}r\delta(r-r_0), \quad F'=F-\tilde{F}.$$

Taking into account (2) and (4) the law for the conservation of angular momentum has the form (see Appendix I for more detail)

$$\frac{\partial}{\partial t}\int_a^b\left(\frac{\partial\Psi}{\partial r}+\frac{r}{2L_0^2}\Psi\right)r^2dr=-\lambda\int_a^b\frac{\partial\Psi}{\partial r}r^2dr+ +\frac{2\Omega}{H_0}I_0\frac{ab}{2}(b^2-a^2)-\frac{\varkappa}{\pi}\frac{r_0^4}{2}. \tag{7}$$

We assume for simplicity that the mean flow is solid body rotation with angular velocity* ω. The ratio ω/Ω is the analog of the Rossby-Blinovaya circulation index for the atmosphere. Under experimental conditions both the rotation of the annular vessel as a whole and also the relative rotation of the fluid within it are clockwise, i.e., the angular velocities Ω and ω are negative. Throughout the text we have given the absolute values for these quantities, and of course the signs have been included in the equations. From Eq. (7) under stationary conditions we have

$$\omega=\frac{4\Omega I_0 ab}{C(a^2+b^2)(2\nu|\Omega|)^{1/2}}-\frac{\varkappa}{8\pi C}\frac{(a+b)^4H_0}{(b^4-a^4)(2\nu|\Omega|)^{1/2}}. \tag{8}$$

The laboratory experiments make it possible to check this relationship and to determine the values for C and $\varkappa$.

Setting $\Psi=\omega r^2/2+\text{const}$, in (6), we arrive at the equation

$$\frac{\partial}{\partial t}\left(\nabla^2\psi'-\frac{1}{L_0^2}\psi'\right)+\omega\frac{\partial\nabla^2\psi'}{\partial\varphi}+\beta\frac{\partial\psi'}{\partial\varphi}=-\lambda\nabla^2\psi'+F'. \tag{9}$$

In the experiments the fluid depth H varies linearly according to the law $H = H_{min} + \text{tg}\,\gamma(r-a)$. We replace the variable β by its mean value, assuming $\beta\approx(2\Omega/H_0r_0)\,\text{tg}\,\gamma$, where $H_0 = H(r_0)$. Further, we use the dimensionless radial coordinate $\rho = r/b$. Equation (9) becomes

$$\left(\frac{\partial}{\partial t}+\omega\frac{\partial}{\partial\varphi}+\lambda\right)\left(\frac{1}{\rho}\frac{\partial}{\partial\rho}\rho\frac{\partial\psi'}{\partial\rho}+\frac{1}{\rho^2}\frac{\partial^2\psi'}{\partial\varphi^2}\right)- -\frac{b^2}{L_0^2}\frac{\partial\psi'}{\partial t}+\beta b^2\frac{\partial\psi'}{\partial\varphi}=b^2F'(\rho,\varphi). \tag{10}$$

We look for a solution of the problem (2) and (10) as a series

*Replacing the zonal flow velocity profile realized in the experiment is more convenient for calculations of the profile in the form of solid-body rotation, and has a slight influence on the spectrum of normal Rossby modes (see Appendix II).

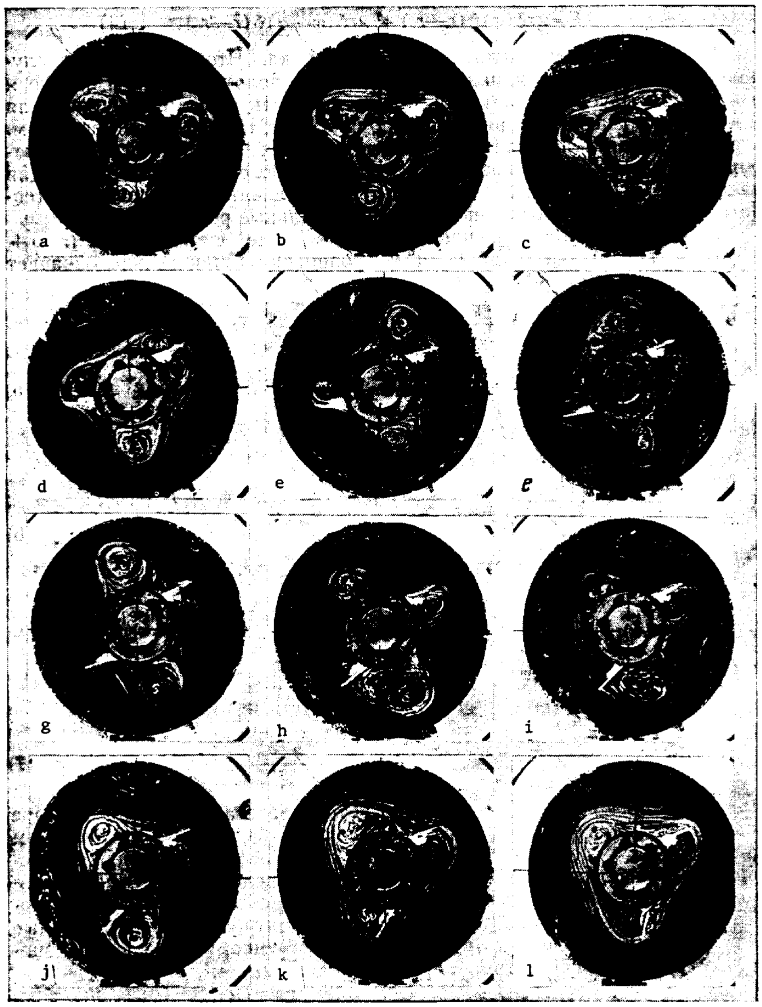

Fig. 5. Transformation of the flow picture past two barriers when α is changed from 113°20' to 238° in steps of 11°20'.

$$\psi' = \sum_{m,n} [A_{mn}(t) \sin m\varphi + B_{mn}(t) \cos m\varphi] Z_m(\mu_{mn}\rho), \quad (11)$$

where the μ_{mn} are the zeroes of the equation (m, n = 1, 2, ...)

$$J_m(\mu) Y_m(\eta\mu) - J_m(\eta\mu) Y_m(\mu) = 0, \ \eta = a/b < 1$$

and the functions

$$Z_m(\mu_{mn}\rho) = Y_m(\mu_{mn}) J_m(\mu_{mn}\rho) - J_m(\mu_{mn}) Y_m(\mu_{mn}\rho)$$

form a complete system of functions that are orthogonal on the segment [η, 1]:

$$\int_\eta^1 Z_m(\mu_{mn}\rho) Z_m(\mu_{mk}\rho) \rho d\rho = \| Z_m \|^2 \delta_{nk},$$

where δ_{nk} is the Kronecker symbol, and

$$\| Z_m(\mu_{mn}\rho) \|^2 = \frac{2}{\pi^2\mu_{mn}^2} \frac{J_m^2(\mu_{mn}\eta) - J_m^2(\mu_{mn})}{J_m^2(\mu_{mn}\eta)}.$$

In these equations J_m and Y_m are m-th order Bessel and Weber functions. Distributing the eddy sources in (10) along the same system of eigenfunctions, we have ($\rho_0 = r_0/b$):

$$(\mu_{mn}^2 + b^2/L_0^2) \frac{dA_{mn}}{dt} - m\omega\mu_{mn}^2 B_{mn} + \beta b^2 m B_{mn} + \lambda\mu_{mn}^2 A_{mn} =$$
$$= -\frac{\varkappa b^2}{\pi} Z_m(\mu_{mn}\rho_0) \rho_0^2 \sin m\alpha \| Z_m(\mu_{mn}\rho) \|^{-2},$$
$$(\mu_{mn}^2 + b^2/L_0^2) \frac{dB_{mn}}{dt} + m\omega\mu_{mn}^2 A_{mn} - \beta b^2 m A_{mn} + \lambda\mu_{mn}^2 B_{mn} =$$

$$= -\frac{\varkappa b^2}{\pi} Z_m(\mu_{mn}\rho_0)\rho_0^2(1+\cos m\alpha)\|Z_m(\mu_{mn}\rho)\|^{-2}.$$

In the stationary case the solution (11) has the form

$$\psi'(\rho, \varphi) = \sum_{m,n} C_{mn}\sin(m\varphi - \varepsilon_{mn}) Z_m(\mu_{mn}\rho),$$

where the amplitude $C_{mn} = (A_{mn}^2 + B_{mn}^2)^{1/2}$ and phase shift relative to the origin $\varepsilon_{mn} = -\operatorname{arctg}(B_{mn}/A_{mn})$ are given by the equations

$$C_{mn} = \frac{2\varkappa b^2 |Z_m(\mu_{mn}\rho_0)|\rho_0^2 \left|\cos\frac{m\alpha}{2}\right|}{\pi\mu_{mn}^2 \|Z_m(\mu_{nm}\rho)\|^2 [\lambda^2 + m^2(\omega - \omega_{mn})^2]^{1/2}},$$

$$\varepsilon_{mn} = -\operatorname{arctg}\left\{\frac{\lambda(1+\cos m\alpha) - m\sin m\alpha(\omega - \omega_{mn})}{\lambda\sin m\alpha + (1+\cos m\alpha)(\omega - \omega_{mn})m}\right\}.$$

Here $\omega_{mn} = \beta b^2/\mu_{mn}^2$ is the phase velocity for the normal Rossby mode taken with opposite sign corresponding to the given set of indices (m, n). The resonance excitation for any normal mode (m, n) can be obtained by changing both the magnitude for ω and also selecting the value for the angle α. The resonance (C_{mn} maximum) is obtained by simultaneously satisfying the conditions

$$\omega = \omega_{mn}, \quad (12)$$

$$m\alpha = 2\pi s, \quad s = 0, \pm 1, \pm 2, \ldots. \quad (13)$$

But if

$$m\alpha = (2s+1)\pi, \quad s = 0, \pm 1, \pm 2, \ldots, \quad (14)$$

then outside of the variation as a function of the values for ω the given normal mode is not excited. For comparison with experiment we limit ourselves to nonzero values for s such that $|\alpha| < 2\pi$.

COMPARISON WITH EXPERIMENT

The results of the previous section make it possible to give a rather clear interpretation of the laboratory observations of the flow around isolated barriers. Waves of maximum extent at right angles to the channel were observed in the experiments, so that $n = 1$ in all the equations.

We turn first to experiments with a single barrier. Assuming that the resonance condition (12) is satisfied and taking (8) into account, we compare the proportion

$$\frac{\mu_{m_1 1}^2}{\mu_{m_2 1}^2} = \sqrt{\frac{\Omega(m_1)}{\Omega(m_2)}\frac{P - S/\Omega(m_1)}{P - S/\Omega(m_2)}}, \quad (15)$$

where $P = 4l_0 ab/C(a^2+b^2)\sqrt{2\nu}$, and $S = \varkappa(a+b)^4 H_0/16\pi C(b^4 - a^4)\sqrt{2\nu}$, the left side of the proportion being determined theoretically and the right side

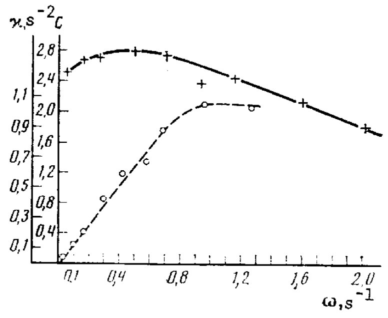

Fig. 6. The dimensionless parameter C (continuous line) and point vorticity source $\varkappa$ (broken line) as a function of the angular rotation rate for the fluid ω when the channel rotates with angular speed Ω = 3.93 sec^{-1}.

being determined experimentally. The values for the dimensionless parameter C and the constant $\varkappa$ are determined from experiment using Eq. (8) by comparing the intensity of the oncoming flow in experiments without a barrier and in experiments with a single barrier. The values computed in this way for C and $\varkappa$ as a function of the angular velocity of the oncoming flow ω (for Ω = 3.93 sec^{-1}) are given in Fig. 6. These values for C and $\varkappa$ are used in Eq. (15) and the calculations are given in Table 1.

Table 2 contains the values for the phase velocity of the Rossby waves ω_{mn} for different wave numbers m and for n = 1 for Ω = 3.93 sec^{-1}, a = 5 cm, b = 14.8 cm, H_0 = 5.61 cm, tg γ' = 0.55 and $\beta = (2\Omega/H_0 r_0)\operatorname{tg}\gamma' = 0.078$ sec^{-1}cm^{-2}. The values for μ_{mn} have been taken from [12]. In [10] a straight channel with an inclined bottom rotating around a vertical axis was used as a simplified theoretical model for the annular vessel. The problems concerning motion in the annular and straight channels are comparable if for the latter restriction is made to the solutions of (1) satisfying the periodicity condition along the length of the channel with period $L = 2\pi r_0$. The computed results for the normal Rossby mode velocities $U_{m1}^* = \beta^*/(\pi^2 D^{-2} + m^2 r_0^{-2})$ for a straight channel L = 62.8 cm long and D = 9.8 cm wide for $\beta^* = (2\Omega/H_0)\operatorname{tg}\gamma' = 0.77$ cm^{-1}sec^{-1} are given in Table 2, which also includes for comparison the linear velocities for the normal Rossby modes U_{ml} in the annular channel calculated for $r = r_0$. The figures show good agreement.

Table 3 gives values for α calculated for different m using Eq. (13) (first column) and Eq. (14) (second column). In our view Table 3 more completely explains the main results of the experiment, particularly the fact that for $\alpha \approx 180°$ a stable four-wave pattern is observed up to the largest values for ω, when favorable

Table 1

$m_1 = 3,\ m_2 = 2$	$m_1 = 5,\ m_2 = 3$	$m_1 = 6,\ m_2 = 5$
1,37	1,79	1,28
1,26	1,56	1,20

Remark. The second column of the table gives values for the left side of the proportion (15) and the third column gives the corresponding values for the right side. The flow rate in the pump for all the experiments was 38 g/sec, and for m = 2, 3, 5 and 6 the angular velocity Ω is 2.06, 3.20, 5.63 and 6.57 sec^{-1}.

Table 2

m	2	3	4	5	6	7
μ_{m1}	5,63	6,58	7,66	8,80	9,95	11,09
ω_{m1}, sec^{-1}	0,576	0,422	0,318	0,236	0,185	0,149
U_{m1}, cm/sec^{-1}	5,70	4,17	3,08	2,34	1,83	1,47
U^*_{m1}, cm/sec^{-1}	5,77	4,25	3,11	2,31	1,76	1,37
U^{**}_{m1}, cm/sec^{-1}	5,49	4,02	2,96	2,25	1,76	1,41
ΔU_{m1} cm/sec^{-1}	1,19	0,79	0,60	0,46	0,38	0,32

Table 3

m			
2	3	4	5
±180° ±90°	±120° ±60°, ±180°	±90°, ±180° ±45°, ±135°	±72°, ±144° ±36°, ±108°, ±180°

conditions are produced for resonance excitation of the wave with $m = 2$. From Table 3 it is also clear why a five-wave system appears when $\alpha \approx 72°$.

When condition (12) is satisfied we have

$$\operatorname{tg} \varepsilon_{m1} = -\operatorname{ctg} \frac{m\alpha}{2}.$$

When α changes through the resonance value $2\pi s/m$ the phase shift decreases abruptly from $-\pi/2$ to $+\pi/2$. This explains the jumping of the eddy from the "windward" to the "leeward" side of the plate which is observed in the experiment. If the condition (12) is satisfied only approximately, then the phase jump condition at π has the form

$$\operatorname{tg} \frac{m\alpha}{2} = -\frac{m(\omega - \omega_{m1})}{\lambda}. \qquad (16)$$

Assuming that the quantity on the right side of (16) is small, we rewrite this condition as

$$\alpha \approx \frac{2\pi s}{m} - \frac{2(\omega - \omega_{m1})}{\lambda}. \qquad (17)$$

A definite asymmetry should thus be observed (relative to the change in the sign for s) for the critical angles $\alpha_{1,2}$ at which there is eddy jumping. For the wave picture with $m = 3$ the experiment shows that $90°40' < \alpha_1 < 102°20'$ and $-133°20' < \alpha_2 < -144°40'$. For the critical angles we take the mean values for α for these intervals: $\alpha_1 = 96°20'$ and $\alpha_2 = -139°$. According to the theoretical Eq. (17), $(|\alpha_1| + |\alpha_2|)/2 = 120$. And in fact from the values for α_1 and α_2 that are given it follows that $(|\alpha_1| + |\alpha_2|)/2 = 117°40'$. Starting from (16), the evaluation of the velocity mismatch $U - U_{31} = r_0(\omega - \omega_{31})$ is straightforward. Setting $\lambda = 0.14\ sec^{-1}$ (for $\nu = 0.01\ cm^2 sec^{-1}$ and $C = 2.79$) and using the values given above for α_1 and α_2, we find respectively $(U - U_{31})_{1,2} =$ 0.33 and 0.25 cm sec^{-1}. It is helpful to compare these values with the half-width for the resonance curves evaluated using the equation $\Delta U_{mn} = \sqrt{3}\mu_{mn} r_0/m$. The corresponding values are given in Table 2. It is seen that in the experiment just now discussed (for which $\Delta U_{31} = 0.79$ cm sec^{-1}) the conditions are very close to resonance.

The authors are grateful to A. M. Obukhov for proposing this research topic, and for his constructive comments and attention to the work.

APPENDIX I

We have the equality

$$\frac{d}{dt}\int_0^{2\pi}\int_a^b\left(\frac{\partial\psi}{\partial r}+\frac{r}{2L_0^2}\psi\right)r^2drd\varphi=-\int_0^{2\pi}\int_a^b\frac{r^2}{2}\frac{\partial}{\partial t}\left(\nabla^2\psi-\frac{1}{L_0^2}\psi\right)rdrd\varphi.$$

The left side can be rewritten as

$$\int_0^{2\pi}\int_a^b\left(r^2\frac{\partial^2\psi}{\partial r\partial t}+\frac{r^3}{2L_0^2}\frac{\partial\psi}{\partial t}\right)drd\varphi=\int_0^{2\pi}\int_a^b\frac{\partial}{\partial r}\left(\frac{r^2}{2}r\frac{\partial^2\psi}{\partial r\partial t}\right)drd\varphi-$$
$$-\int_0^{2\pi}\int_a^b\frac{r^2}{2}\frac{1}{r}\frac{\partial}{\partial r}r\frac{\partial^2\psi}{\partial r\partial t}rdrd\varphi+\int_0^{2\pi}\int_a^b\frac{r^2}{2L_0^2}\frac{\partial\psi}{\partial t}rdrd\varphi.$$

Using the boundary conditions (2) and adding the null integral

$$\int_0^{2\pi}\int_a^b\frac{r^2}{2}\frac{1}{r^2}\frac{\partial^3\psi}{\partial\varphi^2\partial t}rdrd\varphi,$$

we obtain the right side of the equality. If we transform the latter using Eq. (1), carrying out the appropriate integrations by parts using Eq. (2), we arrive at the theorem for the conservation of angular momentum:

$$M=\int_0^{2\pi}\int_a^b\left(\frac{\partial\psi}{\partial r}+\frac{r}{2L_0^2}\psi\right)r^2drd\varphi,$$

$$\frac{dM}{dt}=-\lambda\int_0^{2\pi}\int_a^b\frac{\partial\psi}{\partial r}r^2drd\varphi+\int_0^{2\pi}\int_a^b\frac{r^2}{2}\frac{2\Omega}{H_0}Irdrd\varphi-\int_0^{2\pi}\int_a^b\frac{r^2}{2}Frdrd\varphi. \quad (18)$$

The first term in (18) is the relative angular momentum (to within the accuracy of a constant factor $\rho_f H_0$, where ρ_f is the fluid density); the second term describes the change in the angular momentum because of the redistribution of the fluid mass in the channel.

APPENDIX II

In order to estimate how much the choice of a specific type of profile for the oncoming flow velocity affects the spectrum of normal Rossby modes, as an alternative to the profile with ω = const we take an eddy-free current with the stream function $\Psi=\tau\ln r+\text{const}$ (τ = const). The corresponding velocity profile is realized when the fluid particles moving from the outer wall of the channel to the inner one preserve their initial angular momentum, which to some degree is also observed in the experiment. Considering Eq. (6) with stationary conditions, neglecting friction and eddy sources, we have

$$\tau\frac{\partial}{\partial\varphi}\nabla^2\psi'+\frac{2\Omega\,(dH/dr)\,r}{H}\frac{\partial\psi'}{\partial\varphi}=0.$$

For the case where $H=\text{tg}\,\alpha r$ (which is satisfied to an accuracy within 20 - 30% for the experimental setup), this equation has an exact solution of the form (11) for the condition

$$2\Omega\tau_{mn}^{-1}=\mu_{mn}^2b^{-2}.$$

The corresponding linear velocities for the waves $U_{m1}^{**}=\tau_{m1}/r_0$ (for $r = r_0$) are given in Table 2. They are acceptably close to the previous computed values.

Received July 29, 1986

REFERENCES

1. Smith, R. B. The influence of mountains on the atmosphere. Adv. Geophys., 21, 1979, pp. 27-230.
2. Orographic effects in planetary flows. GARP Publication Series, No. 23. ICSU. WMO, 1980, 450 pp.
3. Taylor, G. I. Experiments with rotating fluids. Proc. Cambridge Phil. Soc., 20, 1921, pp. 326-329.
4. Von Arx, W. S. Some techniques for laboratory study of ocean circulation. Proc. First Sympos. Use Models in Geophys. Fluid Dynamics. Washington, DC, 1953.
5. Antipov, S. V., M. V. Nezlin, V. K. Rodionov, Y. N. Snezhkin and A. S. Trubnikov. Rossby solitons: stability, collisions, asymmetry, and generation by shear currents. ZhETF, 84, 1983, No. 4, pp. 1357-1372.
6. Greenspan, Kh. Teoriya vrashchayushchikhsya zhidkostey (Theory of rotating fluids). Leningrad, Gidrometeoizdat, 1975, 304 pp.
7. Hide, R., A. Ibbetson and M. J. Lighthill.

On slow transverse flow past obstacles in a rapidly rotating fluid. J. Fluid Mech., 32, Pt. 2, 1968, pp. 251-272.

8. Chernous'ko, Yu. L. Experimental investigation of two-dimensional flows with horizontal shear in a rotating channel. Izv. AN SSSR. FAO, 16, No. 4, 1980, pp. 423-427.
9. Dolzhanskiy, F. V. Generation of eddy disturbances on a background of two-dimensional flow with shear excited in a Coriolis force yield by mass sources and sinks. Izv. AN SSSR. FAO, 17, No. 6, 1981, pp. 563-573.
10. Dolzhanskiy, F. V., M. V. Kurganskiy and Yu. L. Chernous'ko. Laboratory and theoretical research on barotropic Rossby waves in a rotating annulus. Izv. AN SSSR. FAO, 15, No. 6, 1979, pp. 597-608.
11. Holton, J. R. An experimental study of forced barotropic Rossby waves. Geophys. Fluid Dyn., 2, No. 4, 1971, pp. 323-342.
12. Weil, J., T. S. Murty and D. B. Rao. Zeroes of $J_n(\lambda)Y_n(\eta\lambda)-J_n(\eta\lambda)\cdot Y_n(\lambda)$. Math. Comp., 21, 1967, pp. 722-727.